Carbohydrate utilization regulator reveals a noncanonical mechanism of nutrient differentiation

Brandon Reyes-Chavez[1,2,#], Joshua D. Kerkaert[1,#], and Lori B. Huberman[1,*]

[1]Plant Pathology and Plant-Microbe Biology Section, School of Integrative Plant Science, Cornell University, Ithaca, NY, USA 14853

[2]Microbiology Department, Cornell University, Ithaca, NY, USA 14853

[#]These authors contributed equally to this work.

*To whom correspondence may be addressed: huberman@cornell.edu

Key words: Carbon catabolite repression, fungi, oleaginous yeast, nutrient sensing, metabolic regulation

ABSTRACT

Cells must sense and respond to nutrients to survive. To efficiently grow in mixed carbon environments, microbes repress genes necessary to utilize carbon sources that require substantial resources to catabolize when a simpler carbon source, such as glucose, is present. This process is known as carbon catabolite repression. Canonically, in fungi, nutrient sensing transcriptional networks are composed of carbon source-specific transcription factors that activate carbon source utilization genes and carbon catabolite repression regulators, which broadly repress all nonpreferred carbon source utilization genes when a preferred carbohydrate is present. In contrast to this model, we identified a transcription factor (Cbr1) in the basidomycete yeast *Rhodotorula* (*Rhodosporidium*) *toruloides* that specifically inhibits glucose-mediated repression of glucose-glucose disaccharide utilization, presenting a mechanism of tailored carbon catabolite repression regulation that combats a negative feedback loop formed when glucose is released during disaccharide utilization. Cbr1 is also required for cellobiose, carboxylic acid, and fucose utilization. Using transcriptomic and molecular analyses, we demonstrated that catabolism of these carbon sources is not metabolically linked, but genes necessary for their utilization are coactivated by Cbr1 in response to each of the carbon sources. This coactivation suggests *R. toruloides* may encounter these carbon sources together, potentially during complex interactions among microbes in nature. Coregulation of nutrient-specific gene activation and carbon catabolite repression by a transcription factor establishes a previously uncharacterized mechanism for building nutrient sensing transcriptional networks in fungi. Characterizing diverse nutrient sensing regulatory mechanisms is critical for understanding resource acquisition during fungal pathogenesis, where carbon catabolite repression is important for virulence and drug tolerance, and metabolically engineering fungi for green biotechnology.

INTRODUCTION

Cells must sense and respond to nutrients to successfully grow and divide using the resources available. For fungi, nutrient sensing is critical to establish fungal colonies, compete with other microbes, and establish pathogenic and symbiotic relationships with plants and animals. Most work characterizing genetic pathways regulating carbon source utilization in fungi has been performed in the Ascomycete phylum [1, 2]. In these fungi, a network of carbon source-specific transcription factors activates genes necessary for utilization of available carbon [3]. However, in a mixed carbon environment, it is not necessarily energetically optimal to simultaneously consume all available carbon sources. Thus, when a more preferred carbon source, such as glucose, is available, a process known as carbon catabolite repression broadly downregulates expression of genes required for utilization of all less preferred carbon sources [1, 3-10].

Many devastating human, animal, and plant pathogens fall outside of the Ascomycete phylum [11]. Genetic mechanisms through which these fungi activate genes necessary to utilize nonpreferred carbon sources and repress these genes in the presence of more preferred carbon sources are significantly less well studied. Basidiomycetes diverged from Ascomycetes approximately 400 million years ago and represent over 30% of described fungi [12, 13]. Recent studies in Basidiomycete pathogens have demonstrated that understanding the regulation of carbon utilization in this phylum is critical, since accurately regulating carbon metabolism is not only important for virulence but also changes the efficacy of antifungal drug treatments [14-16].

To address this knowledge gap, we investigated genetic mechanisms regulating carbon utilization in the basidiomycete yeast *Rhodotorula toruloides* (previously *Rhodosporidium toruloides*). Recent studies of Ascomycete yeast species have established these organisms have a range of carbon utilization repertoires, from specialists capable of consuming only a small range of carbohydrates to generalists that have a much broader carbon utilization repertoire [17]. *R. toruloides* is a generalist that can consume most soluble breakdown products

65 of plant biomass [18, 19]. *R. toruloides* can also accumulate up to 70% of its biomass as fatty
66 acids in conditions in which carbon is abundant but other nutrients are limiting and produces
67 useful secondary metabolites, such as carotenoids [20-26]. This makes *R. toruloides* an
68 excellent choice for metabolic engineering [27], where understanding the regulation of carbon
69 metabolism is critical [28, 29].

70 Cellulose is the most abundant plant biomass component and is composed of glucose
71 chains linked by β-1,4-glycosidic bonds [30]. *R. toruloides* can utilize the disaccharide cellulose
72 building block, cellobiose [31]. We identified a transcription factor, Cbr1, required for cellobiose
73 utilization. Cbr1 is homologous to the cellulose degradation regulator CLR-2/ClrB in
74 Ascomycetes [32], but the role of Cbr1 is significantly expanded in *R. toruloides*, elucidating
75 alternative mechanisms of building carbon utilization regulatory networks in fungi. Unlike CLR-
76 2/ClrB, Cbr1 is also required for tricarboxylic acid (TCA) cycle intermediate and fucose
77 utilization. Cellobiose, fucose, and TCA cycle intermediates are not catabolized through similar
78 pathways, suggesting *R. toruloides* may inhabit an ecological niche in which these carbon
79 sources are frequently found together, potentially through cooperation with or exploitation of
80 saprophytic filamentous fungi.

81 Further investigation of Cbr1 demonstrated this transcription factor inhibits carbon
82 catabolite repression specifically of glucose-glucose disaccharide utilization genes. This role for
83 Cbr1 contrasts with previously identified regulatory mechanisms of carbon catabolite repression,
84 which regulate utilization of all nonpreferred carbon sources. Taken together, the diverse roles of
85 Cbr1 in *R. toruloides* metabolic regulation present a previously uncharacterized mechanism of
86 carbon catabolite repression and nutrient sensing transcriptional network composition in fungi.

87

88 **RESULTS**

89 *Cbr1 is required for wild-type utilization of cellobiose, TCA cycle intermediates, and fucose*

90 *R. toruloides* can utilize cellobiose, the disaccharide breakdown product of the most
91 abundant plant cell wall polysaccharide, cellulose [31]. Several transcription factors regulate
92 cellulose and cellobiose utilization in Ascomycete filamentous fungi, including CLR-1/ClrA, CLR-
93 2/ClrB, and XlnR [1, 32-35]. To investigate genetic mechanisms regulating *R. toruloides*
94 cellobiose utilization, we searched for genes in the *R. toruloides* genome with homology to
95 these transcription factors. No clear homolog of CLR-1/ClrA or XlnR existed in *R. toruloides* (Fig
96 S1). However, we identified a single homolog of CLR-2/ClrB, RTO4_13588 (Fig 1A and Fig S1).
97

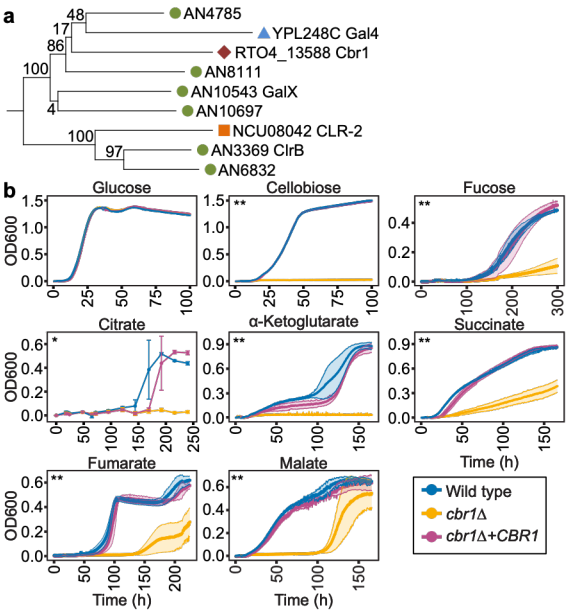

98

99 **Fig 1. *CBR1* (RTO4_13588) is involved in utilization of cellobiose, TCA cycle**
100 **intermediates, and fucose.** (**A**) Protein sequences of *N. crassa* CLR-2 and *Aspergillus*
101 *nidulans* ClrB homologs were used to build a phylogenetic tree using the maximum likelihood
102 method based on the Jones-Taylor-Thornton matrix-based model using FastTree [36]. Numbers
103 at nodes indicate the reliability of each split in the tree as computed using the Shimodaira-
104 Hasegawa test on three alternate topologies around that split with 1,000 resamples. *R.*
105 *toruloides* proteins are indicated with maroon diamonds. *N. crassa* proteins are indicated with
106 orange squares. *A. nidulans* proteins are indicated with green circles. *S. cerevisiae* proteins are

107 indicated with blue triangles. **(B)** Growth curves (OD600) of the indicated strains grown in yeast
108 nitrogen base (YNB) with the indicated carbon source at 1% except for citrate which was at 8.5
109 mM. Lines are the average and bars or colored bands are the standard deviation of three
110 biological replicates. *$p_{adj} < 10^{-4}$ and **$p_{adj} < 10^{-10}$ for *cbr1*Δ vs wild type (WT) and *cbr1*Δ vs
111 *cbr1*Δ + *CBR1* as determined by pairwise comparisons of estimated marginal means with a
112 holm multiple comparison correction.
113
114 We hypothesized RTO4_13588 may play a role in regulating cellobiose utilization in *R.*
115 *toruloides*. To test this hypothesis, we deleted RTO4_13588 and grew the resulting
116 RTO4_13588Δ strain on cellobiose. Growth of cells lacking RTO4_13588 on glucose was
117 indistinguishable from wild type cells (Fig 1B). However, deletion of RTO4_13588 resulted in a
118 complete lack of growth on cellobiose, which could be complemented by exogenous expression
119 of RTO4_13588 (Fig 1B). The *N. crassa* homolog of Cbr1, CLR-2, also plays a role in mannan
120 utilization leading us to hypothesize that *CBR1* may be required for utilizing mannose, a major
121 mannan building block [37], but *cbr1*Δ cells grew as well as wild type on mannose (Fig S2A).
122 The closest homolog to RTO4_13588 in the model yeast *Saccharomyces cerevisiae* is the
123 transcription factor Gal4, which regulates galactose utilization (Fig 1A) [38]. To test whether
124 RTO4_13588 also played a role in regulating galactose utilization in *R. toruloides*, we grew wild
125 type and RTO4_13588Δ cells with galactose as the sole carbon source. There was no
126 detectable difference in growth between wild type cells and cells lacking RTO4_13588 on
127 galactose (Fig S2A). Thus, we named RTO4_13588, *CBR1* for cellobiose regulator 1.
128 *R. toruloides* can grow on a wide variety of soluble carbon sources [18, 31]. We asked
129 whether *CBR1* was required for growth on any additional carbon sources. Cells lacking *CBR1*
130 were unable to grow as well as wild type cells on the deoxy hexose sugar fucose, which could
131 be complemented by exogenous expression of *CBR1* (Fig 1B). The growth of *cbr1*Δ cells was

132 indistinguishable from wild type cells on all other sugars tested (fructose, xylose, arabinose,
133 galacturonic acid, sucrose, maltose, trehalose, and raffinose) and on the lignin phenolic building
134 blocks, coumaric and ferulic acid (Fig S2A-S2B). *CBR1* was not required for utilization of the
135 lipid mimic Tween-80, the fermentation product acetate, or the amino acids L-alanine, proline,
136 glutamate, or glycine, suggesting *cbr1*Δ cells were capable of respiration (Fig S2C-S2D). Thus,
137 we hypothesized *cbr1*Δ cells would be able to grow on TCA cycle intermediates. To our surprise,
138 *cbr1*Δ cells had significant growth defects on citrate, α-ketoglutarate, succinate, fumarate, or
139 malate relative to wild type and *cbr1*Δ + *CBR1* cells (Fig 1B).
140 The role for Cbr1 in TCA cycle intermediate and fucose utilization could either be an
141 expanded role for Cbr1 in *R. toruloides* relative to CLR-2/ClrB or a previously uncharacterized
142 role for CLR-2/ClrB. To distinguish between these two possibilities, we assessed growth of the
143 model filamentous fungus *Neurospora crassa* wild type and Δ*clr-2* cells in media containing
144 succinate, α-ketoglutarate, malate, or fucose as the sole carbon source. Wild type *N. crassa*
145 was only capable of limited growth on TCA cycle intermediates or fucose, and deletion of *clr-2*
146 caused no detectable growth defect (Fig S3). These data suggest the *CBR1* role in regulating
147 TCA cycle intermediate and fucose utilization is an expanded role for this transcription factor,
148 relative to Cbr1 orthologs in Ascomycete filamentous fungi.
149
150 *Cbr1 activates a core regulon of five genes in response to cellobiose, TCA cycle intermediates,*
151 *and fucose*
152 We had three possible hypotheses for genetic mechanisms through which Cbr1 could
153 regulate cellobiose, TCA cycle intermediate, and fucose utilization: (1) Cbr1 regulates genes
154 necessary to utilize all three classes of carbon sources in response to any of these carbon
155 sources, (2) Cbr1 regulates genes necessary to utilize each carbon source only in response to
156 that specific carbon source, and (3) *R. toruloides* utilization of cellobiose, fucose, and/or TCA

157 cycle intermediates proceeds through atypical metabolic pathways that require the same
158 transporters and/or catabolic enzymes. To distinguish between these three hypotheses, we
159 used transcriptional profiling. We exposed wild type and *cbr1*Δ cells to yeast nitrogen base
160 (YNB) lacking a carbon source (no carbon) or supplemented with 1% cellobiose, fucose, or
161 succinate for 8 h prior to harvesting the cells for RNA sequencing (RNAseq). The cellobiose,
162 succinate, and no carbon samples were submitted for whole transcript RNAseq, and the fucose
163 samples were submitted for 3' RNAseq.

164 Given the limited transcriptional characterization of *R. toruloides* on cellobiose or
165 succinate, we first examined the transcriptional profile of wild type cells in these conditions
166 relative to carbon starvation. The expression of 1168 genes was at least four-fold differentially
167 expressed in wild type cells exposed to cellobiose compared to carbon starvation, with 155
168 genes upregulated and 1013 genes downregulated. In wild type cells exposed to succinate, 525
169 genes were at least four-fold differentially expressed relative to carbon starved cells, with 142
170 genes upregulated and 383 genes downregulated. Intriguingly, over 75% of genes differentially
171 expressed on succinate (405/525) were also differentially expressed on cellobiose, supporting
172 the hypothesis that similar sets of genes are regulated in response to cellobiose and succinate
173 (Fig S4A-C and Dataset S1-S2).

174 Cells lacking *CBR1* also showed substantial transcriptional responses to cellobiose and
175 succinate compared to carbon starvation. Five hundred seventy-nine genes were at least four-
176 fold differentially expressed in cellobiose compared to carbon starvation. Eighty-one of the 179
177 genes (45%) upregulated on cellobiose in *cbr1*Δ cells were also upregulated in wild type cells
178 exposed to cellobiose, and 319 of the 400 genes (80%) downregulated on cellobiose in *cbr1*Δ
179 cells had the same expression pattern in wild type cells (Fig S4A, S4D, S4F, and Dataset S1-
180 S2). Similarly, 742 genes were differentially expressed on succinate compared to carbon
181 starvation in *cbr1*Δ cells. Eighty-six of the 296 genes (29%) upregulated on succinate in *cbr1*Δ

182 cells were also upregulated in wild type cells exposed to succinate, and 256 of 446 genes (57%)
183 downregulated on succinate in *cbr1*Δ cells were also downregulated in wild type cells exposed
184 to succinate (Fig S4B, S4E, S4G, and Dataset S1-S2). The significant transcriptional response
185 to cellobiose and succinate combined with the high degree of transcriptional similarity exhibited
186 by *cbr1*Δ and wild type cells suggests despite not being able to utilize cellobiose or succinate
187 like wild type cells, *cbr1*Δ cells still respond to these carbon sources to some extent.

188 Although many fungal transcription factor genes are upregulated in the condition in
189 which the transcription factor plays a role, *CBR1* expression was not induced in response to
190 cellobiose or succinate compared to carbon starvation (Fig S5A and Dataset S1-S2). To directly
191 regulate gene expression, Cbr1 must be present in the nucleus. We hypothesized Cbr1 might
192 be transported into the nucleus under conditions where it plays a role. To test this hypothesis,
193 we tagged Cbr1 with green fluorescent protein (mEGFP) and the histone H2A subunit *HTA1*
194 (RTO4_12090) with mRuby2 and exposed these cells to carbon starvation, glucose, cellobiose,
195 or succinate to identify the localization of Cbr1. Cbr1 colocalized with the histone H2A subunit
196 under all four conditions, indicating Cbr1 is expressed and in the nucleus during exposure to
197 glucose, cellobiose, succinate, and carbon starvation (Fig S5B).

198 To gain insight into the mechanism behind the growth defects of cells lacking *CBR1*, we
199 examined genes decreased in expression in *cbr1*Δ relative to wild type cells. Using a four-fold
200 differential expression cutoff, 284, 18, 25, and 25 genes were downregulated in *cbr1*Δ compared
201 to wild type cells on cellobiose, succinate, carbon starvation, and fucose, respectively (Fig 2A-D
202 and Dataset S1-S2). In concordance with our hypothesis that cellobiose, carboxylic acid, and
203 fucose utilization are transcriptionally linked via *CBR1*, genes annotated as part of the Kyoto
204 Encyclopedia of Genes and Genomes (KEGG) [39] 2-oxocarboxylic acid metabolism category
205 were enriched in the *CBR1* regulon on cellobiose (Fig 2E). Carbohydrate metabolism KEGG
206 [39] and gene ontology (GO) [40, 41] related categories were enriched on succinate, no carbon,

207 and fucose. Further analysis revealed the carbohydrate-related enrichments primarily consisted

208 of genes predicted to encode β-glucosidases, which cleave cellobiose into two glucose

209 molecules (Fig 2E). Only five genes were differentially expressed by at least four-fold in at least

210 three of the four conditions: two encoding putative β-glucosidases (RTO4_16716 and

211 RTO4_16717) that are adjacent in the *R. toruloides* genome, two encoding putative major

212 facilitator superfamily transporters (RTO4_10339 and RTO4_13825), and one encoding a

213 putative phosphoglycerate mutase (RTO4_11229) (Fig 2A-D and Dataset S1-S2).

214

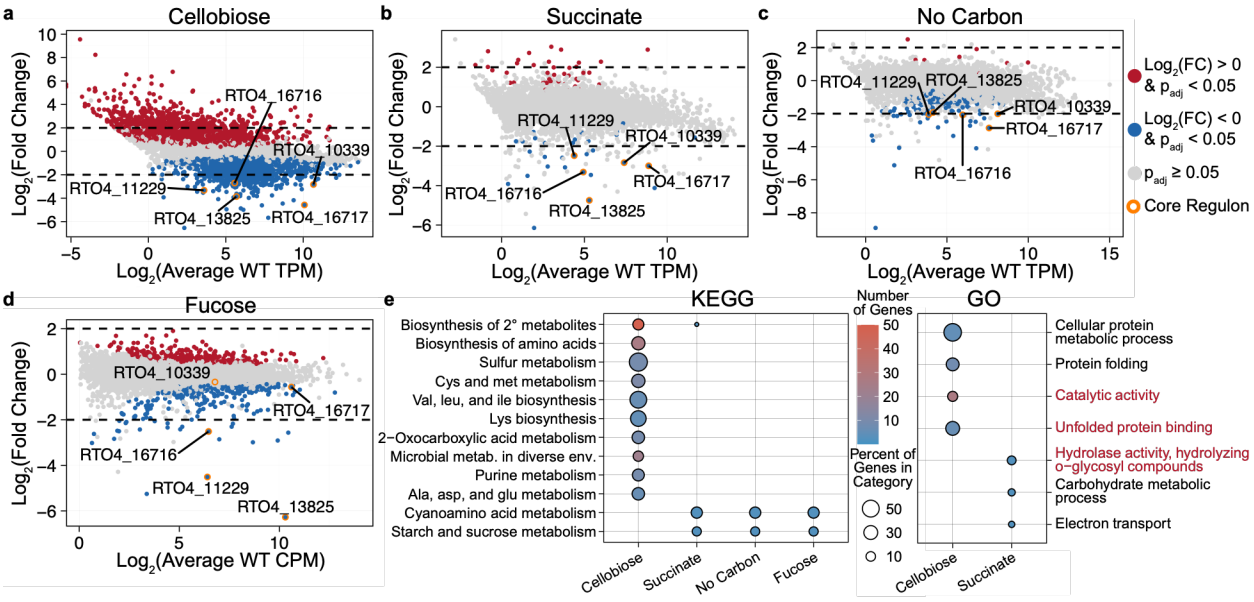

215

216 **Fig 2. Cbr1 regulates a core regulon of five genes.** (**A-D**) Scatterplots of the $\log_2$(average

217 expression) of all genes in wild type (WT) cells versus the $\log_2$(fold change) in gene expression

218 in *cbr1*Δ relative to wild type cells when cells were exposed to (**A**) cellobiose, (**B**) succinate, (**C**)

219 media lacking a carbon source, or (**D**) fucose. Genes with $p_{adj} < 0.05$ are indicated in red or blue

220 if they had higher or lower expression in *cbr1*Δ cells than wild type cells, respectively. Genes

221 differentially expressed by a least four-fold in at least three of the four conditions (*CBR1* core

222 regulon) are circled in orange and labeled with their protein IDs. Genes in grey were not

223 significantly differentially expressed in *cbr1*Δ relative to wild type cells. Black dotted lines

224 indicate four-fold differential expression. Standard RNAseq (**A-C**) was used to determine gene
225 expression in transcripts per million (TPM) and fold change during exposure to cellobiose,
226 succinate, and carbon starvation. 3'RNAseq (**D**) was used to determine gene expression in
227 counts per million (CPM) and fold change during exposure to fucose. (**E**) Genes expressed at
228 least four-fold lower in *cbr1*Δ cells than wild type cells for each carbon source were tested for
229 Kyoto Encyclopedia of Genes and Genomes (KEGG) [39] (left) and gene ontology (GO) [40, 41]
230 (right) functional category enrichment. Comparisons were only displayed if they had at least one
231 statistically significantly enriched category for each analysis. Dot color represents the number of
232 genes differentially expressed belonging to a given category. Dot size represents the percent of
233 genes belonging to a given category that were differentially expressed relative to all genes in
234 that category. The text of GO biological process and molecular function categories are colored
235 black and red, respectively. The expression of *CBR1* was left out of the scatterplots, KEGG, and
236 GO enrichment analyses, since the change in expression of this gene was due to its deletion in
237 the *cbr1*Δ strain. All RNAseq experiments had three biological replicates.
238
239 *Cbr1-regulated β-glucosidases are necessary for cellobiose utilization*
240 The *CBR1*-dependent expression of two predicted β-glucosidase genes led us to
241 hypothesize that one or both β-glucosidase genes is essential for cellobiose utilization. An
242 amino acid alignment using LALIGN [42] revealed 72% identity and 90% similarity between the
243 two proteins, suggesting a potential for redundancy, so to test this hypothesis we deleted
244 RTO4_16716 and RTO4_16717, together and individually. RTO4_16716Δ RTO4_16717Δ cells
245 grew like wild type cells on glucose, citrate, succinate, and fucose, but were unable to grow on
246 cellobiose (Fig 3A and Fig S6A). Analysis of the individual deletion mutants revealed that
247 deletion of RTO4_16717 alone eliminated growth on cellobiose and complementation with
248 RTO4_16717 restored the ability to grow on cellobiose (Fig 3B). Cells lacking RTO4_16716

249 alone grew as well as wild type cells on cellobiose (Fig 3B). These data indicate RTO4_16717

250 encodes the primary β-glucosidase for cellobiose utilization. Thus, we named RTO4_16717 and

251 RTO4_16716, *BGL1* and *BGL2*, respectively, for β-glucosidase 1 and 2.

252

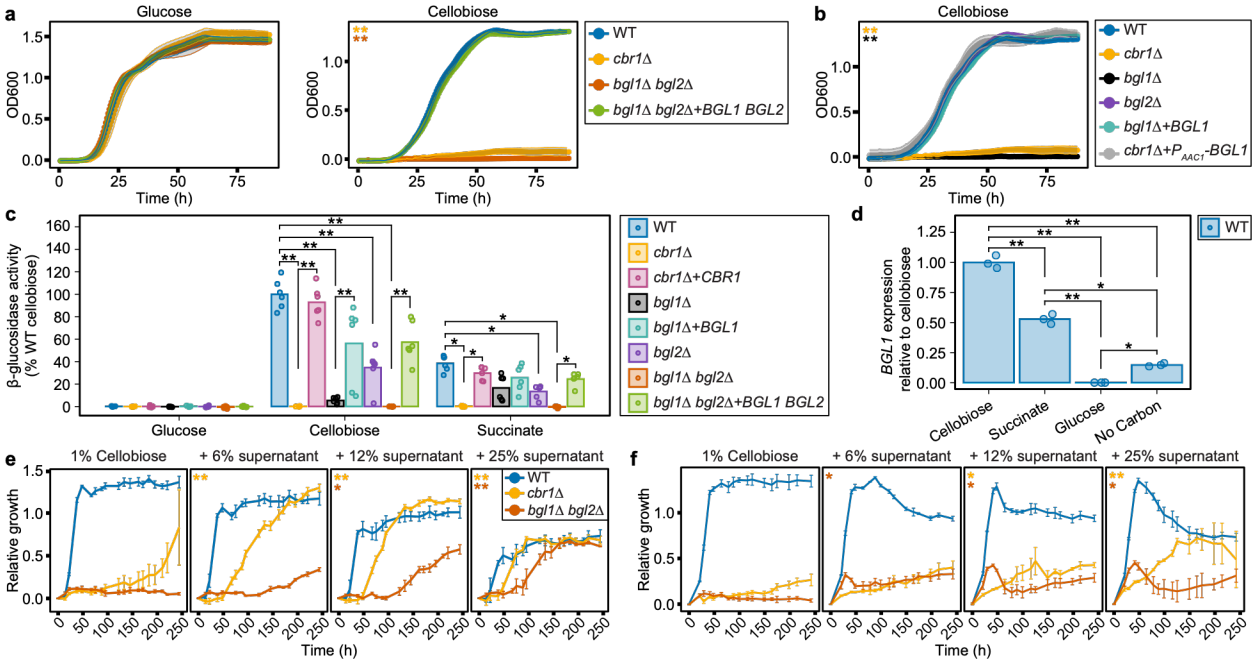

253

254 **Fig 3. Cbr1-dependent expression of secreted β-glucosidase genes *BGL1* (RTO4_16717)**

255 **and *BGL2* (RTO4_16716) is necessary for cellobiose utilization.** (**A-B**) Growth (OD600) of

256 the indicated strains in the indicated carbon sources. (**C**) β-glucosidase activity secreted by the

257 indicated strains into culture supernatants after 20 h growth on the indicated carbon sources. β-

258 glucosidase activity is normalized to the β-glucosidase activity of wild type (WT) cells on

259 cellobiose. Growth (OD600) at time of supernatant harvest is in Fig S6B. (**D**) *BGL1* expression

260 of WT cells exposed to the indicated carbon source for 4 h relative to *BGL1* expression during

261 exposure to cellobiose for 4 h. (**E-F**) Normalized growth (OD600) of the indicated strains in 1%

262 cellobiose supplemented with the indicated percentage of spent supernatant from wild type cells

263 grown in (**E**) 1% cellobiose or (**F**) 1% succinate. To account for growth on nutrients remaining in

264 the spent supernatant, growth was normalized by subtracting the growth of each replicate on

265 media lacking a carbon source supplemented with the same concentration of spent supernatant.
266 Growth curves without normalization, growth curves in media without a carbon source
267 supplemented with spent supernatants, and β-glucosidase activity present in spent
268 supernatants are in Fig S7. (**A**, **B**, **E**, and **F**) Lines are the average and bars or colored bands
269 are the standard deviation of three biological replicates. (**C** and **D**) Bars are the average and
270 dots are the individual data points of (**C**) five (*cbr1*Δ) or six (all other strains) biological replicates
271 or (**D**) three biological replicates. (**A** and **B**) Colored stars indicate a significant difference in
272 growth of the respectively colored strain compared to wild type cells and, when applicable, the
273 respective complement strain. (**E** and **F**) Colored stars indicate a significant difference in growth
274 of the respectively colored strain compared to growth of that strain without supernatant
275 supplementation. *$p_{adj} < 0.05$ and **$p_{adj} < 10^{-7}$ as determined by either (**A**, **B**, **E**, and **F**) pairwise
276 comparisons of estimated marginal means with a holm multiple comparison correction, (**C**) a
277 two-way ANOVA with a TukeyHSD post-hoc test, or (**D**) a one-way ANOVA with a TukeyHSD
278 post-hoc test.
279
280 Both *BGL1* and *BGL2* have predicted secretion signals, leading us to hypothesize
281 cellobiose cleavage by β-glucosidases occurs extracellularly. To address this hypothesis, we
282 harvested supernatants of wild type, *cbr1*Δ, and *cbr1*Δ + *CBR1* cell cultures after 20 h of growth
283 in glucose, cellobiose, or succinate to measure secreted β-glucosidase activity. β-glucosidase
284 activity was detected in the culture supernatant of wild type cells exposed to cellobiose
285 indicating that β-glucosidases are indeed secreted by *R. toruloides* (Fig 3C). Consistent with our
286 transcriptomics data, and despite the lack of a role for *BGL1* and *BGL2* in carboxylic acid
287 utilization (Fig S6A), β-glucosidase activity was also detectable in the culture supernatant of wild
288 type cells on succinate. Deletion of *CBR1* eliminated β-glucosidase activity in the supernatant of
289 cellobiose and succinate cultures. This activity was restored in the supernatant of cultures of

290 *cbr1*Δ + *CBR1* cells, indicating the secreted β-glucosidase activity was dependent on *CBR1* (Fig
291 3C).

292 Glucose cultures had no detectable β-glucosidase activity, which could either be due to
293 reduced expression of β-glucosidase genes or reduced secretion of β-glucosidase proteins in
294 glucose relative to cellobiose and succinate media (Fig 3C). To distinguish between these
295 possibilities, we performed reverse transcription quantitative PCR (RT-qPCR) on *BGL1* in wild
296 type cells. Corroborating our RNAseq data, *BGL1* expression was highest on cellobiose,
297 followed by succinate, and then carbon starvation (Fig 3D). During exposure to glucose, *BGL1*
298 expression was nearly undetectable, indicating the lack of β-glucosidase activity in the glucose
299 culture supernatant was due to reduced expression of β-glucosidase genes (Fig 3C and 3D).
300 These data may indicate β-glucosidase expression is regulated by carbon catabolite repression
301 and that β-glucosidases potentially act as "scout" enzymes during carbon starvation similar to
302 some polysaccharide degrading enzymes in some filamentous fungi [1, 3].

303 Given that *bgl1*Δ cells cannot grow when cellobiose is the sole carbon source (Fig 3B),
304 we hypothesized Bgl1 was the source of the secreted β-glucosidase activity. To test this
305 hypothesis, we incubated *bgl1*Δ cells in cellobiose, succinate, or glucose for 20 h. While β-
306 glucosidase activity in the cellobiose *bgl1*Δ culture supernatant was 22-fold lower than that of
307 wild type culture supernatants, it was detectable, and β-glucosidase activity of succinate *bgl1*Δ
308 cultures was even more pronounced (Fig 3C and Fig S6C). This reduction in β-glucosidase
309 secretion was mitigated in *bgl1*Δ + *BGL1* cells (Fig 3C). The low level of β-glucosidase activity
310 remaining in *bgl1*Δ cells could either result from secretion of Bgl2 or an unidentified protein. To
311 distinguish between these possibilities, we exposed *bgl1*Δ *bgl2*Δ and *bgl1*Δ *bgl2*Δ + *BGL1 BGL2*
312 cells to cellobiose, succinate, or glucose for 20 h. Cells lacking both *BGL1* and *BGL2* had no
313 detectable β-glucosidase activity, which was rescued by complementation with *BGL1* and *BGL2*
314 (Fig 3C and Fig S6C). These data suggested Bgl2 contributes to β-glucosidase activity in

315 cellobiose and succinate cultures even though *BGL2* was dispensable for growth on cellobiose.
316 Indeed, cells lacking *BGL2* alone had a 2.8-fold reduction of β-glucosidase activity on both
317 cellobiose and succinate relative to wild type cells, demonstrating that both Bgl1 and Bgl2 are
318 responsible for the secreted β-glucosidase activity of *R. toruloides* (Fig 3C).

319 It was possible either that β-glucosidase genes were the only Cbr1-regulated genes
320 necessary for cellobiose utilization or that other genes were also required. To distinguish
321 between these two possibilities, we expressed *BGL1* under the constitutive *AAC1*
322 (RTO4_12704) promoter [43] in a *cbr1*Δ background (*cbr1*Δ + P_{AAC1}-*BGL1*). Constitutive
323 expression of *BGL1* in *cbr1*Δ cells resulted in wild type levels of growth on cellobiose when cells
324 were inoculated at very low densities and a growth advantage on cellobiose relative to wild type
325 cells at higher starting densities (Fig 3B and Fig S6D and S6E). Correspondingly, *cbr1*Δ + P_{AAC1}-
326 *BGL1* cellobiose culture supernatants had 3.2-fold higher β-glucosidase activity than wild type
327 culture supernatants (Fig S6F).

328 If β-glucosidase activity is the only Cbr1-regulated requirement for cellobiose utilization,
329 we speculated *cbr1*Δ and *bgl1*Δ *bgl2*Δ cell growth on cellobiose could be rescued by
330 exogenously supplied β-glucosidases. To test this hypothesis, we inoculated wild type, *cbr1*Δ,
331 and *bgl1*Δ *bgl2*Δ cells into cellobiose supplemented with filtered, spent supernatant from wild
332 type cells grown on cellobiose, succinate, or glucose. This spent supernatant supplementation
333 enabled significantly improved growth of *cbr1*Δ and *bgl1*Δ *bgl2*Δ cells, which was not due to
334 growth on residual carbon in the spent supernatant (Fig 3E, 3F, and Fig S7). Our data
335 demonstrate genes encoding secreted β-glucosidases, activated in response to cellobiose and
336 TCA cycle intermediates, are the only Cbr1-regulated requirement for cellobiose utilization.
337

338 *CBR1-mediated transcriptional response to cellobiose is dependent on extracellular β-*
339 *glucosidases*

340 Extracellular degradation of cellobiose by *R. toruloides* provoked the question of whether
341 cellobiose activates the *CBR1*-dependent transcriptional response to cellobiose or if the
342 activating signal is a cellobiose catabolic derivative. We differentiated between these
343 possibilities in two ways.
344 We first compared the transcriptional profile of *bgl1*Δ *bgl2*Δ cells exposed to cellobiose,
345 which have no extracellular β-glucosidase activity but contain wild type copies of *CBR1*, to that
346 of wild type and *cbr1*Δ cells using 3' RNAseq. The transcriptional profiles of *bgl1*Δ *bgl2*Δ cells
347 were more similar to *cbr1*Δ than wild type cells (Fig 4A-C and Fig S8 and Dataset S3-S4).
348 Thirty-five genes were at least four-fold differentially expressed in *bgl1*Δ *bgl2*Δ relative to wild
349 type cells (12 upregulated and 23 downregulated) (Fig 4A and Dataset S3-S4). Twenty-three of
350 these genes were also at least four-fold differentially expressed in *cbr1*Δ compared to wild type
351 cells (Fig 4B and Dataset S3-S4). In contrast, only five genes were at least four-fold differentially
352 expressed in *bgl1*Δ *bgl2*Δ relative to *cbr1*Δ cells, which included a 38-fold upregulation of the
353 *CBR1*-regulated predicted transporter gene RTO4_13825 (Fig 4C and Dataset S3-S4). The
354 expression pattern of RTO4_13825, raised the question of whether any other genes in the core
355 Cbr1 regulon were involved in cellobiose sensing or utilization. Cells lacking RTO4_13825,
356 RTO4_10339, or RTO4_11229 all grew as well as wild type on cellobiose (Fig S9). These data
357 indicate the signal for the *CBR1*-dependent cellobiose response requires secreted β-
358 glucosidases, suggesting cellobiose is likely not the signaling molecule for Cbr1 activation.
359

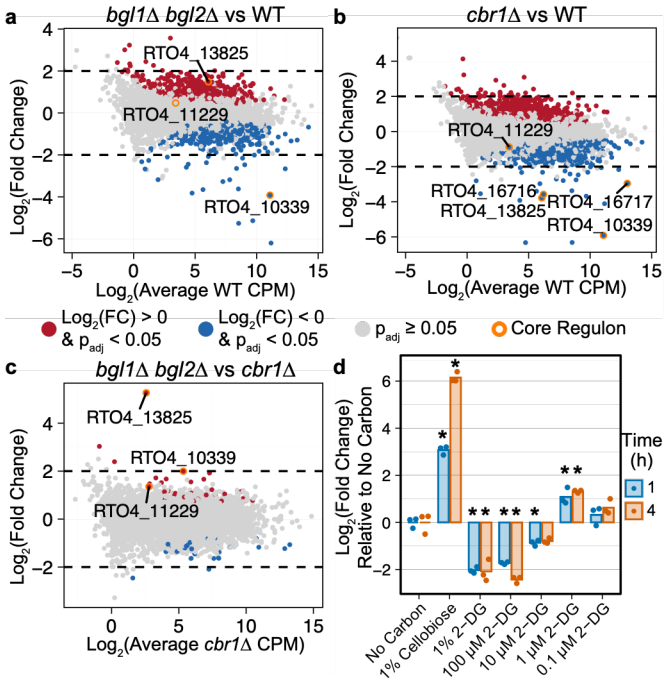

Fig 4. *CBR1*-mediated transcriptional response to cellobiose is dependent on secreted β-glucosidases. (**A-C**) Scatterplots of the $\log_2$(average expression) of all genes in (**A-B**) wild type (WT) or (**C**) *cbr1*Δ cells versus the $\log_2$(fold change) in gene expression for the indicated comparison when cells were exposed to cellobiose as measured by 3'RNAseq. Genes with p_{adj} < 0.05 are indicated in red or blue if they had higher or lower expression, respectively, in (**A** and **C**) *bgl1*Δ *bgl2*Δ cells or (**B**) *cbr1*Δ cells. The genes in the *CBR1* core regulon are circled in orange and labeled with their respective protein IDs. The expression of *CBR1*, *BGL1,* and *BGL2* were left out of the scatterplots involving their respective deletion strains. RNAseq experiments had three biological replicates. (**D**) *BGL1* expression in wild type cells exposed to carbon starvation for 1 h followed by exposure to continued carbon starvation or the indicated concentrations of cellobiose or 2-deoxyglucose (2-DG) as the sole carbon source for 1 h or 4 h. Expression values were normalized to the average expression of *BGL1* on no carbon for each timepoint and $\log_2$ transformed. Bars are the average and dots are the values of three biological replicates. *p_{adj} < 0.05 relative to the no carbon condition for the respective time point, as determined by two-way ANOVA with a TukeyHSD post-hoc test.

376

377 β-glucosidases cleave cellobiose into two glucose molecules. Thus, a second way we
378 answered the question of whether cellobiose or a cellobiose catabolic derivative is the activation
379 signal was to determine whether low glucose concentrations activated Cbr1-regulated gene
380 expression. To mitigate changes in glucose concentration due to metabolism, we used the non-
381 metabolizable glucose analog 2-deoxyglucose. We exposed wild type cells to 10-fold dilutions of
382 2-deoxyglucose (100 μM to 0.1 μM), 1% 2-deoxyglucose, 1% cellobiose, or carbon starvation
383 for 1 h and 4 h and measured *BGL1* transcription via RT-qPCR. As expected, cells exposed to
384 cellobiose expressed *BGL1* at high levels, and *BGL1* expression was repressed during
385 exposure to 1% 2-deoxyglucose (Fig 4D). Exposure to 1 μM 2-deoxyglucose resulted in a two to
386 three-fold increase in *BGL1* expression relative to carbon starvation at both timepoints (Fig 4D).
387 This *BGL1* activation did not rise to the same magnitude as exposure to cellobiose itself,
388 perhaps due to differences in glucose concentration, the rate glucose enters the cell, or a lack of
389 resources due to starvation on 2-deoxyglucose. However, increased *BGL1* expression on 1 μM
390 2-deoxyglucose suggests a low concentration of glucose, a catabolic cellobiose derivative,
391 activates β-glucosidase expression.

392

393 *A Cbr1-regulated transporter gene is necessary for citrate utilization*

394 Two genes encoding predicted major facilitator superfamily transporters (RTO4_13825
395 and RTO4_10339) and a gene encoding a predicted phosphoglycerate mutase (RTO4_11229)
396 were also members of the *CBR1* core regulon. We hypothesized these genes may be
397 necessary for growth on TCA cycle intermediates and/or fucose. To test this hypothesis, we
398 grew RTO4_13825Δ, RTO4_10339Δ, and RTO4_11229Δ cells on media containing glucose,
399 fucose, citrate, succinate, α-ketoglutarate, malate, or fumarate. The growth of RTO4_10339Δ
400 and RTO4_11229Δ cells was indistinguishable from wild type cells under all conditions tested

401 (Fig S9). Cells lacking RTO4_13825 were unable to grow on citrate but grew as well as wild

402 type cells on all other carbon sources tested (Fig 5A and Fig S9A). Thus, we named

403 RTO4_13825 *TCT1* for tricarboxylic acid transporter.

404

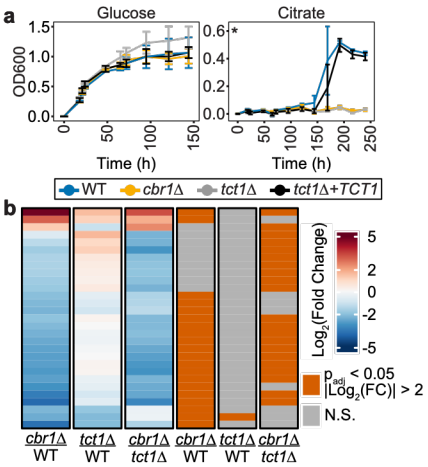

405

406 **Fig 5. *TCT1* (RTO4_13825) is required for citrate utilization.** (**A**) Growth (OD600) of the

407 indicated strains in YNB 1% glucose or 8.5 mM citrate. Lines are the average and bars are the

408 standard deviation of three biological replicates. *$p_{adj} < 10^{-7}$ of *cbr1*Δ vs wild type (WT), *tct1*Δ vs

409 WT, and *tct1*Δ vs *tct1*Δ + *TCT1* as determined by pairwise comparisons of estimated marginal

410 means with a holm multiple comparison correction. (**B**) Heatmap of the log_2(fold change) in the

411 expression of genes at least four-fold differentially expressed in one or more of the indicated

412 comparisons when cells were exposed to citrate as the sole carbon source, as measured by

413 3'RNAseq. Orange bars to the right of the heatmap indicate significance using the criteria of p_{adj}

414 < 0.05 and at least four-fold change in expression, while grey bars indicate genes that do not

415 meet those criteria in the indicated comparison (N.S., not significant). The expression of *CBR1*

416 and *TCT1* were left out of the heatmaps since changes in expression were due to their

417 respective deletions in the *cbr1*Δ and *tct1*Δ strains. RNAseq experiments had three biological

418 replicates.

419

420

421 To gain further insight into the role of *TCT1*, we conducted RNAseq on wild type, *cbr1*Δ,
422 and *tct1*Δ cells exposed to citrate for 24 h. Only 20 genes were at least four-fold differentially
423 expressed in *cbr1*Δ relative to wild type cells (Fig 5B and Dataset S5-S6). Surprisingly, these 20
424 genes did not include *TCT1* or genes predicted to play a role in citrate metabolism. Of the other
425 genes in the *CBR1* core regulon, *BGL1* and *BGL2* were downregulated by 6.7 and 3.2-fold,
426 respectively, in *cbr1*Δ relative to wild type cells, but RTO4_10339 and RTO4_11229 were not
427 differentially expressed (Fig 5B and Dataset S5-S6). Only one gene, RTO4_15140, had
428 decreased expression in *tct1*Δ cells relative to wild type cells. RTO4_15140 was also
429 downregulated in *cbr1*Δ relative to wild type cells (Fig 5B and Dataset S5-S6). RTO4_15140 is
430 predicted to encode a P-type ATPase transduction domain A containing protein with a single
431 transmembrane domain, and any potential role in citrate utilization is unclear. The similarity of
432 *tct1*Δ and wild type cell transcriptional profiles may suggest *tct1*Δ cells can sense citrate, despite
433 not being able to grow.

434

435 *Cbr1 inhibits carbon catabolite repression during glucose-glucose disaccharide utilization*

436 Glucose is a highly preferred carbon source in most fungi. Extracellular β-glucosidases
437 cleave cellobiose into two glucose molecules, which we hypothesized would repress cellobiose
438 utilization genes via carbon catabolite repression [1, 3, 4]. *BGL1* expression is almost
439 undetectable when wild type cells are exposed to 1% glucose or at least 100 μM 2-
440 deoxyglucose (Fig 3D and 4D). Thus, we hypothesized wild type cell growth on cellobiose would
441 be inhibited by the non-hydrolyzable glucose analog 2-deoxyglucose. Indeed, 61 μM 2-
442 deoxyglucose fully inhibited *R. toruloides* growth on 1% cellobiose, indicating glucose is
443 preferred over cellobiose by *R. toruloides* (Fig 6A).

444

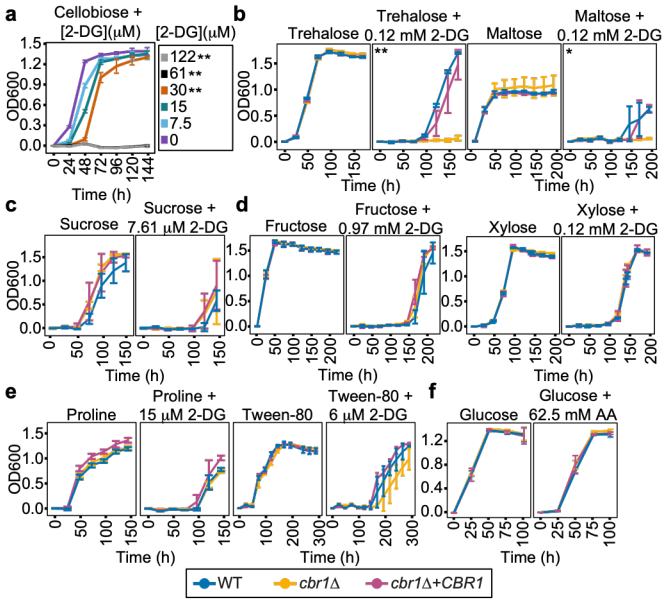

Fig 6. Cbr1 inhibits carbon catabolite repression during glucose-glucose disaccharide utilization. (**A**) Growth (OD600) of wild type (WT) cells in 1% cellobiose supplemented with the indicated concentration of 2-deoxyglucose (2-DG). (**B-F**) Growth of the indicated strains on the indicated carbon sources with the indicated concentration of 2-DG or allyl alcohol (AA). Lines are the average and bars are the standard deviation of (**A-E**) three or (**F**) four biological replicates. *$p_{adj} < 0.01$ and **$p_{adj} < 10^{-4}$ for (**A**) 1% cellobiose supplemented with the indicated 2-DG concentration vs 1% cellobiose or (**B-F**) *cbr1*Δ vs WT and *cbr1*Δ vs *cbr1*Δ + *CBR1* as determined by pairwise comparisons of estimated marginal means with a holm multiple comparison correction.

This carbon preference represents a biological challenge during utilization of substrates in which glucose is released during catabolism; a negative feedback loop could repress substrate utilization genes in response to the released glucose, slowing growth on the carbon source. We hypothesized *CBR1* may inhibit carbon catabolite repression to bypass this negative feedback loop. To test this hypothesis, we grew wild type, *cbr1*Δ, and *cbr1*Δ + *CBR1* cells on a nonpreferred carbon source and 2-deoxyglucose. Cells lacking *CBR1* were significantly more

462 sensitive to 2-deoxyglucose than wild type or *cbr1*Δ + *CBR1* cells when the glucose-glucose
463 disaccharides maltose or trehalose were the carbon source, suggesting Cbr1 is a negative
464 regulator of carbon catabolite repression (Fig 6B).

465 Canonically, regulators of carbon catabolite repression regulate a broad spectrum of
466 nonpreferred carbon source utilization genes [1, 3-10]. We hypothesized *CBR1* would play a
467 similar role in *R. toruloides*. However, the growth of *cbr1*Δ cells exposed to 2-deoxyglucose in
468 combination with the glucose-fructose disaccharide sucrose, the hexose monosaccharide
469 fructose, the pentose monosaccharide xylose, the amino acid proline, or the lipid mimic Tween-
470 80 was indistinguishable from wild type cells (Fig 6C-6E). To measure the role of *CBR1* in
471 regulating genes involved in alcohol utilization, we used allyl alcohol, which is converted to the
472 toxic molecule acrolein by alcohol dehydrogenases. Alcohol dehydrogenase expression is
473 repressed by glucose [44]. Wild type and *cbr1*Δ cells were equally sensitive to allyl alcohol,
474 indicating glucose-mediated repression of alcohol dehydrogenases is not dependent on Cbr1
475 (Fig 6F). To determine whether any *CBR1* core regulon genes play a role in carbon catabolite
476 repression, we tested 2-deoxyglucose sensitivity of *bgl1*Δ *bgl2*Δ, *tct1*Δ, RTO4_10339Δ, and
477 RTO4_11229Δ cells. The sensitivity of these strains to 2-deoxyglucose during exposure to
478 trehalose, maltose, sucrose, proline, xylose, fructose, and tween-80 was indistinguishable from
479 wild type cells (Fig S10). These data indicate Cbr1 inhibits carbon catabolite repression of
480 glucose-glucose disaccharides either by directly regulating gene expression or through genes
481 outside of the *CBR1* core regulon.

482 A role for Cbr1 Ascomycete homologs in carbon catabolite repression regulation has not
483 been identified, so we asked whether the *N. crassa* Cbr1 homolog CLR-2 plays a similar role.
484 The sensitivity of wild type and Δ*clr-2* cells to 2-deoxyglucose was indistinguishable during
485 growth on the glucose-glucose disaccharide trehalose or the monosaccharide xylose (Fig S11).
486 These data indicate the role for Cbr1 in *R. toruloides* in inhibiting carbon catabolite repression of

487 glucose-glucose disaccharides is an expanded role for Cbr1 relative to the model Ascomycete
488 ortholog CLR-2.
489
490 **DISCUSSION**
491 Gene regulation in response to nutrient availability requires cells to integrate information
492 from activating and repressing nutrient signals. Previously described fungal transcriptional
493 networks regulating carbon utilization are made up of carbon source-specific transcription
494 factors that activate genes necessary to utilize a particular carbon source when it is present and
495 broad-acting transcription factors that regulate carbon catabolite repression [1, 2]. However,
496 studies of these carbon source utilization transcriptional networks have mainly focused on
497 Ascomycete fungi. We investigated nutrient sensing regulatory mechanisms in a Basidiomycete
498 yeast and identified a transcription factor that coregulates carbon source-specific gene
499 activation and carbon catabolite repression specifically of glucose-glucose disaccharide
500 utilization genes (Fig 7).
501

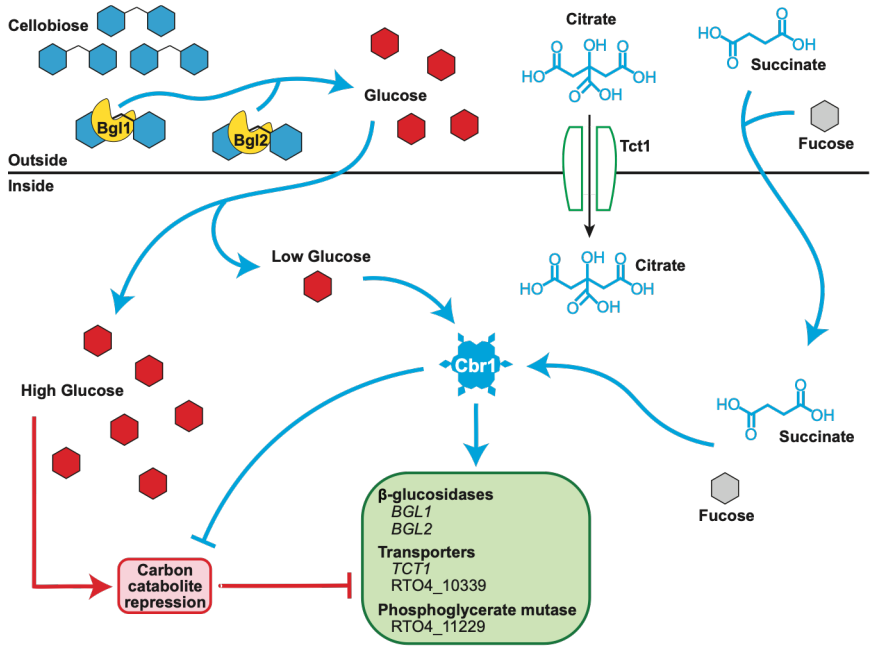

502

503 **Fig 7. Model for Cbr1-mediated regulation of cellobiose, TCA cycle intermediate, and**
504 **fucose utilization and carbon catabolite repression.** Cbr1 is activated by the presence of a
505 low glucose concentration, fucose, and TCA cycle intermediates or their metabolic derivatives.
506 Activated Cbr1 induces the expression of genes encoding β-glucosidases, predicted
507 transporters, and a predicted phosphoglycerate mutase. The Cbr1-regulated predicted
508 transporter gene *TCT1* is required for citrate utilization. Tct1 is placed at the plasma membrane
509 in this model, but the localization of Tct1 is currently unknown and should be the subject of
510 future studies. Transporters for other TCA cycle intermediates and fucose are unknown. The β-
511 glucosidase genes *BGL1* and *BGL2* encode secreted β-glucosidases that cleave cellobiose into
512 two glucose molecules. *BGL1* is required for growth on cellobiose. A high glucose concentration
513 activates carbon catabolite repression, which represses β-glucosidase gene expression and
514 likely represses the expression of genes necessary to utilize fucose and TCA cycle
515 intermediates. Cbr1 plays a role in inhibiting carbon catabolite repression, specifically when a
516 glucose-glucose disaccharide is present as the nonpreferred carbon source.
517
518 *Cbr1 regulation of cellobiose, TCA cycle intermediate, and fucose utilization may shed light on*
519 *complex microbial interactions*
520 There have been limited investigations of genetic regulators of cellulose and cellobiose
521 utilization in Basidiomycetes. A recent study identified Roc1 as a regulator of cellulase-encoding
522 genes in the basidiomycete wood-decaying fungus *Schizophyllum commune* [45]. However,
523 homologs of Roc1 do not exist outside of the Agaricomycetes [45]. In *Ganoderma lucidum*, the
524 R2R3-type MYB transcription factor *Gl*Myb activates cellulase gene expression [46]. In
525 Ascomycete filamentous fungi, CLR-2/ClrB regulates cellulose degradation and utilization
526 through direct activation of cellulase genes [32, 47]. We identified the CLR-2/ClrB ortholog Cbr1
527 in the oleaginous, basidiomycete yeast *R. toruloides* (Fig 1). Although Ascomycete and
528 Basidiomycete fungi are separated by approximately 400 million years of evolution [12], Cbr1 is

529 required to utilize the cellulose breakdown product cellobiose (Fig 1). *N. crassa* CLR-2 does not
530 directly regulate the expression of genes encoding β-glucosidases, which are regulated by CLR-
531 1 [32, 47]. However, although the role of Cbr1 is significantly expanded beyond that of CLR-
532 2/ClrB to include inhibition of carbon catabolite repression and utilization of TCA cycle
533 intermediates and fucose, Cbr1 regulation of cellobiose utilization indicates some functional
534 conservation of CLR-2/ClrB/Cbr1 exists between Ascomycete filamentous fungi and
535 Basidiomycete yeast.

536 Cbr1 regulates citrate utilization through the predicted transporter gene *TCT1* and
537 cellobiose utilization through the β-glucosidase genes *BGL1* and *BGL2* (Fig 7). Genetic
538 mechanisms through which Cbr1 regulates utilization of fucose and dicarboxylic acid TCA cycle
539 intermediates remains unclear. It is possible the two uncharacterized genes in the *CBR1* core
540 regulon, the predicted transporter RTO4_10339 and the predicted phosphoglycerate mutase
541 RTO4_11229, play roles in fucose and/or dicarboxylic acid utilization that are redundant with
542 other *CBR1*-regulated genes that did not meet our strict *CBR1* core regulon criteria (Fig 2 and
543 Fig S4). It will be the role of future studies to characterize roles for RTO4_10339, RTO4_11229,
544 and other genes that may be responsible for fucose and dicarboxylic acid catabolism in the
545 *CBR1* pathway.

546 In other fungal species, utilization of multiple carbon sources is occasionally regulated by
547 a single transcription factor. CLR-2 in *N. crassa* regulates cellulose utilization, mannan
548 utilization, and a small number of hemicellulose utilization genes [3, 32, 37, 47]. In *Trichoderma*
549 *reesei*, *Penicillium oxalicum*, and some Aspergilli, the transcription factor Xyr1/XlnR regulates
550 cellulose and hemicellulose utilization [33-35]. ARA-1/Ara1 regulates arabinan and galactose
551 utilization in *N. crassa* and *T. reesei* [3, 48]. FarA regulates utilization of fatty acids and the lignin
552 component ferulic acid in Aspergilli [49, 50]. In *Candida albicans*, Adr1 is required for growth on
553 citrate and substrates that feed into the TCA cycle, like glutamate and malate [51]. However, in

554 these examples linkage of these carbon sources can be explained either by the presence of
555 both carbon sources in the plant cell wall (i.e., cellulose and hemicellulose or arabinan and
556 galactose) or shared catabolic pathways (i.e., fatty acids and ferulic acid or citrate, glutamate,
557 and malate).

558 Cellobiose, fucose, and TCA cycle intermediates are not linked by known catabolic
559 pathways, and our data do not support catabolism through the same noncanonical metabolic
560 pathway in *R. toruloides*. Cbr1-regulated β-glucosidase genes are critical for cellobiose but not
561 fucose or TCA cycle intermediate utilization (Fig 3 and Fig S6A), while Tct1 is necessary for
562 citrate but not cellobiose or fucose utilization (Fig 5A and Fig S9A). Aside from *CBR1*, we did not
563 identify genes necessary for utilization of all three of cellobiose, fucose, and TCA cycle
564 intermediates.

565 We speculate coregulation of cellobiose, fucose, and TCA cycle intermediates may
566 suggest *R. toruloides* encounters cellobiose, fucose, and TCA cycle intermediates together in
567 nature. One possible explanation is *R. toruloides* scavenges cellobiose and fucose during plant
568 biomass degradation by filamentous fungi, which secrete organic acids like citrate or succinate
569 to acidify their environment and can contain fucose in their cell walls [52-54]. β-glucosidase
570 gene activation that is primed by organic acids secreted by fungi or fucose in fungal cell walls
571 before encountering cellobiose released from cellulose could confer a growth advantage to *R.*
572 *toruloides* over microbes that only activate β-glucosidase genes in response to cellobiose itself.
573 Indeed, high densities of cells constitutively expressing *BGL1* that do not require time to activate
574 β-glucosidase genes had a growth advantage over wild type cells that activated β-glucosidase
575 genes in response to cellobiose (Fig S6D).

576

577 *Cbr1 regulation of carbon catabolite repression specifically of glucose-glucose disaccharides*
578 *disrupts a negative feedback loop for disaccharide utilization*

579 Carbon catabolite repression enables prioritization of carbon sources that require less
580 energy to metabolize over carbon sources that require more energy to metabolize [1]. Known
581 carbon catabolite repression genetic mechanisms regulate genes required for utilization of all
582 less preferred carbon sources when a more preferred carbon source is present [3-10]. In
583 contrast, Cbr1 inhibits carbon catabolite repression specifically of glucose-glucose disaccharide
584 utilization (Fig 6). We speculate this mechanism allows continued expression of genes that
585 hydrolyze disaccharide bonds even when this hydrolysis produces preferred monosaccharides,
586 combating a negative feedback loop (Fig 7). To our knowledge, genetic linkage via a single
587 transcription factor of carbon catabolite repression inhibition with activation of genes necessary
588 for nonpreferred carbon source utilization has not been described in fungi. Additionally,
589 regulation of genes involved in utilization of a specific class of nonpreferred carbon sources in
590 response to a preferred carbon source represents a previously uncharacterized form of carbon
591 catabolite repression regulation.
592 Fungal pathogens of plants and animals that do not regulate carbon catabolite
593 repression like wild type cells frequently have reduced virulence [8, 55-57]. Carbon utilization
594 and carbon catabolite repression regulation by fungi also affects how they respond to antifungal
595 drugs [14, 15]. Thus, understanding diverse carbon catabolite repression mechanisms present
596 throughout the fungal kingdom is critical in controlling fungal disease. Additionally, a more
597 complete understanding of mechanisms of carbon catabolite repression and the diversity of
598 nutrient sensing transcriptional networks is necessary for harnessing the primary and secondary
599 metabolic capabilities of the fungal kingdom for biotechnology. Mapping these networks will be
600 critical in metabolically engineering fungi for green industrial fermentation.
601
602 **MATERIALS and METHODS**
603 *Strains and culturing*

604 *R. toruloides* strains used in this study are listed in Table S1. All strains were derived
605 from the wild type reference strain IFO 0880 (also called NBRC 0880, obtained from Biological
606 Resource Center, NITE (NBRC), Japan). The starting strain for genetic manipulations was the
607 non-homologous end-joining deficient *yku70*Δ (RTO4_11920Δ) strain [58]. *R. toruloides* was
608 transformed using *Agrobacterium tumefaciens*-mediated transformation as previously described
609 [26], using *A. tumefaciens* EHA 105 and plasmids derived from pGI2 [59]. All strains were
610 confirmed by PCR and/or DNA sequencing of transformed loci. For details see Text S1. *R.*
611 *toruloides* strains were grown from freezer stocks on yeast extract peptone dextrose (YPD)
612 (VWR) + 2% agar (BD Difco™ Bacto™) plates at 28°C for 2-3 d prior to inoculation into liquid
613 YPD to grow strains at 28°C with constant shaking at 250 rpm to exponential phase growth prior
614 to starting experiments.
615 *N. crassa* strains used in this study are listed in Table S2. These strains were derived
616 from the wild type reference strain FGSC 2489 and obtained from the Fungal Genetics Stock
617 Center [60, 61]. *N. crassa* cells were grown from freezer stocks on Vogel's minimal medium [62]
618 + 2% sucrose + 1.5% agar (BD Difco™ Bacto™) slants for 2 d at 28°C in the dark and 4 d at
619 28°C in constant light. *N. crassa* conidia were harvested from slants with sterile double distilled
620 H_2O for inoculation.
621 All *R. toruloides* experiments were performed with yeast nitrogen base (YNB) with
622 NH_4SO_4 without amino acids (MP Biomedicals) + 12 mM K_2HPO_4 (Fisher) + 38 mM KH_2PO_4
623 (Fisher) + 100 nM Fe(II)SO_4 pH 6.2 with the indicated carbon source at 1% w/v with the
624 exception of coumaric acid and ferulic acid, which were added at a concentration of 0.2% w/v,
625 and citrate which was added at a concentration of 8.5 mM. All *N. crassa* experiments were
626 performed using Vogel's minimal medium [62] with 50 mM NH_4Cl instead of 25 mM NH_4NO_3
627 (VMM NH_4Cl) and the indicated carbon source at 1% w/v. Carbon sources used are listed in
628 Table S3.
629

630 *R. toruloides and N. crassa growth experiments*

631 *R. toruloides* colonies were inoculated into liquid YPD and grown at 28°C with constant
632 shaking at 250 rpm to exponential phase. Cells were then washed and inoculated into 750 μL of
633 the indicated media in 48-well plates at 0.01 OD600/mL or 0.1 OD600/mL, except for the growth
634 curve in Fig S6D, which was inoculated at 0.5 OD600/mL as measured by an Eppendorf
635 BioPhotometer with a 10 mm path length. Plates were incubated at 28°C with constant shaking
636 (3 mm orbit, 600 rpm for individual time points and 3 mm orbit, 425 rpm for kinetic growth
637 experiments). Growth was measured as OD600 on an Agilent BioTek Synergy HTX for
638 individual time points or an Agilent BioTek Epoch2 for kinetic growth experiments. For details
639 see Text S1.

640 *N. crassa* conidia were inoculated into either 100 mL of liquid VMM NH_4Cl with the
641 indicated carbon source in 250 mL flasks or 3 mL of liquid VMM NH_4Cl with the indicated carbon
642 source in round-bottomed, deep-well 24-well plates. After 24 h (flasks) or 7-10 d (24-well plates)
643 biomass was harvested, dried for 24 h in a 60°C drying oven, and weighed. For details see Text
644 S1.

645

646 *Phylogenetic tree generation*

647 The Basic Local Alignment Search Tool for proteins (BLASTP) was used to identify
648 homologs of CLR-1, CLR-2, and XLR-1 from *N. crassa* (OR74A) and ClrA, ClrB, and XlnR from
649 *Aspergillus nidulans* (A4) in the proteomes of *N. crassa*, *A. nidulans*, *S. cerevisiae* (S288C), and
650 *R. toruloides* (IFO 0880). CLR-1, CLR-2, and XLR-1 from *N. crassa* (OR74A) and ClrA, ClrB,
651 and XlnR from *A. nidulans* (A4) protein sequences were obtained from Mycocosm [63].
652 Homologs with $E < 10^{-10}$ were aligned via MUSCLE [64] in MEGA11 [65] and the phylogenetic
653 tree was generated using FastTree [36] using the maximum likelihood method based on the
654 Jones-Taylor-Thornton matrix-based model and visualized in MEGA11. The reliability of each

655 split in the tree was computed using the Shimodaira-Hasegawa test on three alternate
656 topologies around that split. Trees were visualized in MEGA11 [65] and rooted on the midpoint.
657
658 *Microscopy*
659 Fluorescent microscopy was performed using a Nikon Eclipse Ti2-E inverted microscope
660 equipped with a prime BSI express CMOS camera using a CFI Plan Apochromat 100X oil
661 objective. For details see Text S1.
662
663 *RNA sequencing and transcript abundance*
664 Flasks containing 100 mL of YNB without a carbon source or YNB with the indicated
665 carbon source were inoculated with the indicated exponentially growing cells at 0.1 OD600/mL
666 (measured by an Eppendorf BioPhotometer). Culture conditions and sequencing methods for
667 each dataset are summarized in Table S4. Cells were harvested and flash frozen in liquid N_2.
668 RNA was extracted using the Quick-RNA Fungal/Bacterial Miniprep Kit (Zymo), followed by
669 either treatment with the TURBO DNA-free kit (Invitrogen) for standard RNAseq or DNase I
670 treatment (NEB) and purification with the Monarch® Spin RNA Cleanup Kit (NEB) for 3'RNAseq.
671 Standard RNAseq was performed at the California Institute for Quantitative Biosciences at the
672 University of California Berkeley (QB3-Berkeley) on an Illumina NextSeq 2000 with 150 bp
673 paired end reads. 3'RNAseq was performed at the Biotechnology Resource Center at Cornell
674 University on an Illumina NovaSeqX with 150 bp paired end reads.
675 Reads were aligned to the *R. toruloides* IFO 0880 genome (v4) [26]. For standard
676 RNAseq, transcript abundance (transcripts per million, TPM) was quantified using Salmon v.
677 1.10.0 [66]. For 3'RNAseq, reads were aligned using STAR v. 2.7.11b [67], counted with HTSeq
678 v. 2.0.9 [68], and counts per million (CPM) values were calculated by dividing counts for a gene
679 by total counts for the sample and multiplying by 10^6. The GFF file used to analyze 3'RNAseq
680 data is available in Dataset S7. Differential expression was determined using DESeq2 v. 1.50.1

681 [69]. RNAseq data were deposited in the Gene Expression Omnibus (GEO) at the National
682 Center for Biotechnology Information (NCBI) and are accessible through GEO series accession
683 numbers GSE293943 (standard RNAseq) and GSE313844 (3'RNAseq). For details see Text
684 S1.
685
686 *Functional enrichment analysis*
687 KEGG and GO enrichment analyses were performed using the enricher function of the
688 clusterProfiler R package v. 4.18.1 with Benjamini-Hochberg multiple hypothesis testing
689 correction [70]. For details see Text S1.
690
691 *Reverse transcription quantitative PCR*
692 To measure *BGL1* expression, wild type cells were exposed to the indicated carbon
693 source in 100 mL of the indicated media in 250 mL flasks and incubated at 28°C with shaking at
694 200 rpm for the indicated length of time. Cells were harvested, flash frozen in liquid N_2, and RNA
695 was purified as described above. RT-qPCR was performed using the Luna® Universal One-Step
696 RT-qPCR Kit (NEB) on a CFX96™ Real-Time System (Bio-Rad). For details see Text S1.
697
698 *β-glucosidase enzyme activity assays*
699 β-glucosidase activity was measured using p-nitrophenyl-β-D-glucopyranoside (EMD
700 Millipore Corp.). For details see Text S1.
701
702 *Spent media growth assays*
703 Filtered supernatants of wild type cells growing in YNB 1% glucose, YNB 1% cellobiose,
704 or YNB 1% succinate were added to YNB lacking a carbon source or YNB 1% cellobiose at the
705 indicated concentration. The indicated strains were inoculated into this media at 0.01 OD600/mL

706 (measured by an Eppendorf BioPhotometer) in 750 μL in 48-well plates and incubated at 28ºC
707 with shaking at 600 rpm (3 mm orbit). For details see Text S1.
708
709 *Statistical significance tests*
710 All statistical analyses were performed in Rstudio (v2025.09.2+418; R v4.5.2) using
711 either a one-way or two-way ANOVA with a Tukey post-hoc test (bar graphs), a two-tailed
712 Welch's two-sample *t*-test (bar graphs), or a general linear model with two-tailed post-hoc
713 analysis using the emmeans function of the emmeans R package [71] with a holm multiple
714 comparison correction (line graphs). Statistical significance for differential expression of
715 RNAseq data was determined using DESeq2 [69]. All experiments were performed with a
716 minimum of three biological replicates. The exact number of replicates for each experiment is
717 noted in the relevant figure legend.
718
719 *Data availability*
720 Raw RNAseq data is available in GEO at the NCBI through accession numbers
721 GSE293943 (standard RNAseq) and GSE313844 (3'RNAseq). Processed RNAseq data is
722 available in Dataset S1-S6. The numerical values used to generate all other graphs are in
723 Dataset S9. Strains constructed in this study are available upon request.
724
725 **ACKNOWLEDGEMENTS**
726 We thank members of the Huberman lab for helpful comments on the manuscript. This
727 work was supported by a grant from the National Institute of General Medical Sciences of the
728 National Institutes of Health (NIH) under Award Number R35GM150926 to L.B.H. J.D.K. was
729 supported by NIH Ruth L. Kirschstein National Research Service Award Institutional Research
730 Training Grant 5T32AI145821-03. This work utilized the Cornell Institute of Biotechnology
731 Biotechnology Resource Center Genomics Facility (RRID:SCR_021727) and BioHPC

732 (RRID:SCR_021757) and the QB3 Genomics core at the University of California Berkeley

733 (RRID:SCR_022170).

734 **REFERENCES**

735 1. Kerkaert JD, Huberman LB. Regulation of nutrient utilization in filamentous fungi. Appl
736 Microbiol Biotechnol. 2023;107(19):5873-98. Epub 2023/08/04. doi: 10.1007/s00253-023-
737 12680-4. PubMed PMID: 37540250; PubMed Central PMCID: PMCPMC10983054.

738 2. Benocci T, Aguilar-Pontes MV, Zhou M, Seiboth B, de Vries RP. Regulators of plant
739 biomass degradation in ascomycetous fungi. Biotechnol Biofuels. 2017;10:152. Epub
740 2017/06/16. doi: 10.1186/s13068-017-0841-x. PubMed PMID: 28616076; PubMed Central
741 PMCID: PMCPMC5468973.

742 3. Wu VW, Thieme N, Huberman LB, Dietschmann A, Kowbel DJ, Lee J, et al. The
743 regulatory and transcriptional landscape associated with carbon utilization in a filamentous
744 fungus. Proc Natl Acad Sci U S A. 2020;117(11):6003-13. Epub 2020/03/01. doi:
745 10.1073/pnas.1915611117. PubMed PMID: 32111691; PubMed Central PMCID:
746 PMCPMC7084071.

747 4. Adnan M, Zheng W, Islam W, Arif M, Abubakar YS, Wang Z, et al. Carbon catabolite
748 repression in filamentous fungi. Int J Mol Sci. 2017;19(1). Epub 2018/01/04. doi:
749 10.3390/ijms19010048. PubMed PMID: 29295552; PubMed Central PMCID:
750 PMCPMC5795998.

751 5. Nehlin JO, Ronne H. Yeast *MIG1* repressor is related to the mammalian early growth
752 response and Wilms' tumour finger proteins. EMBO J. 1990;9(9):2891-8. Epub 1990/09/01.
753 PubMed PMID: 2167835; PubMed Central PMCID: PMC552004.

754 6. Arst HN, Jr., Cove DJ. Nitrogen metabolite repression in *Aspergillus nidulans*. Mol Gen
755 Genet. 1973;126(2):111-41. Epub 1973/11/02. doi: 10.1007/bf00330988. PubMed PMID:
756 4591376.

757 7. Dowzer CE, Kelly JM. Analysis of the *creA* gene, a regulator of carbon catabolite
758 repression in *Aspergillus nidulans*. Mol Cell Biol. 1991;11(11):5701-9. Epub 1991/11/01.
759 PubMed PMID: 1922072; PubMed Central PMCID: PMC361941.

760 8. Hong Y, Cai R, Guo J, Zhong Z, Bao J, Wang Z, et al. Carbon catabolite repressor
761 MoCreA is required for the asexual development and pathogenicity of the rice blast fungus.
762 Fungal Genet Biol. 2021;146:103496. Epub 2020/12/09. doi: 10.1016/j.fgb.2020.103496.
763 PubMed PMID: 33290821.
764 9. Strauss J, Mach RL, Zeilinger S, Hartler G, Stöffler G, Wolschek M, et al. Cre1, the
765 carbon catabolite repressor protein from *Trichoderma reesei*. FEBS Lett. 1995;376(1-2):103-7.
766 Epub 1995/11/27. doi: 10.1016/0014-5793(95)01255-5. PubMed PMID: 8521952.
767 10. Sun J, Glass NL. Identification of the CRE-1 cellulolytic regulon in *Neurospora crassa*.
768 PloS One. 2011;6(9):e25654.
769 11. Li Y, Steenwyk JL, Chang Y, Wang Y, James TY, Stajich JE, et al. A genome-scale
770 phylogeny of the kingdom Fungi. Curr Biol. 2021;31(8):1653-65.e5. Epub 20210218. doi:
771 10.1016/j.cub.2021.01.074. PubMed PMID: 33607033; PubMed Central PMCID:
772 PMCPMC8347878.
773 12. Taylor JW, Berbee ML. Dating divergences in the Fungal Tree of Life: review and new
774 analyses. Mycologia. 2006;98(6):838-49. doi: 10.3852/mycologia.98.6.838. PubMed PMID:
775 17486961.
776 13. Ainsworth GC. Ainsworth & Bisby's dictionary of the fungi: Cabi; 2008.
777 14. Chen L, Tian X, Zhang L, Wang W, Hu P, Ma Z, et al. Brain glucose induces tolerance of
778 *Cryptococcus neoformans* to amphotericin B during meningitis. Nat Microbiol. 2024;9(2):346-58.
779 Epub 20240115. doi: 10.1038/s41564-023-01561-1. PubMed PMID: 38225460.
780 15. Caza M, Hu G, Price M, Perfect JR, Kronstad JW. The zinc finger protein Mig1 regulates
781 mitochondrial function and azole drug susceptibility in the pathogenic fungus *Cryptococcus*
782 *neoformans*. mSphere. 2016;1(1). Epub 2016/06/16. doi: 10.1128/mSphere.00080-15. PubMed
783 PMID: 27303693; PubMed Central PMCID: PMCPMC4863601.
784 16. Price MS, Betancourt-Quiroz M, Price JL, Toffaletti DL, Vora H, Hu G, et al.
785 *Cryptococcus neoformans* requires a functional glycolytic pathway for disease but not

786 persistence in the host. mBio. 2011;2(3):e00103-11. Epub 2011/06/10. doi:
787 10.1128/mBio.00103-11. PubMed PMID: 21652778; PubMed Central PMCID:
788 PMCPMC3110414.
789 17. Opulente DA, LaBella AL, Harrison MC, Wolters JF, Liu C, Li Y, et al. Genomic factors
790 shape carbon and nitrogen metabolic niche breadth across Saccharomycotina yeasts. Science.
791 2024;384(6694):eadj4503. Epub 20240426. doi: 10.1126/science.adj4503. PubMed PMID:
792 38662846; PubMed Central PMCID: PMCPMC11298794.
793 18. Kim J, Coradetti ST, Kim YM, Gao Y, Yaegashi J, Zucker JD, et al. Multi-omics driven
794 metabolic network reconstruction and analysis of lignocellulosic carbon utilization in
795 *Rhodosporidium toruloides*. Front Bioeng Biotechnol. 2020;8:612832. Epub 2021/02/16. doi:
796 10.3389/fbioe.2020.612832. PubMed PMID: 33585414; PubMed Central PMCID:
797 PMCPMC7873862.
798 19. Yaegashi J, Kirby J, Ito M, Sun J, Dutta T, Mirsiaghi M, et al. *Rhodosporidium toruloides*:
799 a new platform organism for conversion of lignocellulose into terpene biofuels and bioproducts.
800 Biotechnol Biofuels. 2017;10:241. Epub 2017/10/28. doi: 10.1186/s13068-017-0927-5. PubMed
801 PMID: 29075325; PubMed Central PMCID: PMCPMC5651578.
802 20. Wiebe MG, Koivuranta K, Penttilä M, Ruohonen L. Lipid production in batch and fed-
803 batch cultures of *Rhodosporidium toruloides* from 5 and 6 carbon carbohydrates. BMC
804 Biotechnol. 2012;12:26. Epub 2012/06/01. doi: 10.1186/1472-6750-12-26. PubMed PMID:
805 22646156; PubMed Central PMCID: PMCPMC3499381.
806 21. Wu S, Hu C, Jin G, Zhao X, Zhao ZK. Phosphate-limitation mediated lipid production by
807 *Rhodosporidium toruloides*. Bioresour Technol. 2010;101(15):6124-9. Epub 2010/03/24. doi:
808 10.1016/j.biortech.2010.02.111. PubMed PMID: 20307977.
809 22. Wu S, Zhao X, Shen H, Wang Q, Zhao ZK. Microbial lipid production by *Rhodosporidium*
810 *toruloides* under sulfate-limited conditions. Bioresour Technol. 2011;102(2):1803-7. Epub
811 2010/10/12. doi: 10.1016/j.biortech.2010.09.033. PubMed PMID: 20934330.

812 23. Zhu Z, Zhang S, Liu H, Shen H, Lin X, Yang F, et al. A multi-omic map of the lipid-
813 producing yeast *Rhodosporidium toruloides*. Nat Commun. 2012;3:1112. Epub 2012/10/11. doi:
814 10.1038/ncomms2112. PubMed PMID: 23047670; PubMed Central PMCID: PMCPMC3493640.
815 24. Lee JJ, Chen L, Shi J, Trzcinski A, Chen WN. Metabolomic profiling of *Rhodosporidium*
816 *toruloides* grown on glycerol for carotenoid production during different growth phases. J Agric
817 Food Chem. 2014;62(41):10203-9. Epub 2014/09/26. doi: 10.1021/jf502987q. PubMed PMID:
818 25254328.
819 25. Mata-Gómez LC, Montañez JC, Méndez-Zavala A, Aguilar CN. Biotechnological
820 production of carotenoids by yeasts: an overview. Microb Cell Fact. 2014;13:12. Epub
821 2014/01/22. doi: 10.1186/1475-2859-13-12. PubMed PMID: 24443802; PubMed Central
822 PMCID: PMCPMC3922794.
823 26. Coradetti ST, Pinel D, Geiselman GM, Ito M, Mondo SJ, Reilly MC, et al. Functional
824 genomics of lipid metabolism in the oleaginous yeast *Rhodosporidium toruloides*. Elife.
825 2018;7:e32110. Epub 2018/03/10. doi: 10.7554/eLife.32110. PubMed PMID: 29521624;
826 PubMed Central PMCID: PMCPMC5922974.
827 27. Park YK, Nicaud JM, Ledesma-Amaro R. The engineering potential of *Rhodosporidium*
828 *toruloides* as a workhorse for biotechnological applications. Trends Biotechnol. 2018;36(3):304-
829 17. Epub 2017/11/15. doi: 10.1016/j.tibtech.2017.10.013. PubMed PMID: 29132754.
830 28. Qin N, Li L, Ji X, Pereira R, Chen Y, Yin S, et al. Flux regulation through glycolysis and
831 respiration is balanced by inositol pyrophosphates in yeast. Cell. 2023;186(4):748-63.e15. Epub
832 20230208. doi: 10.1016/j.cell.2023.01.014. PubMed PMID: 36758548.
833 29. Yu T, Liu Q, Wang X, Liu X, Chen Y, Nielsen J. Metabolic reconfiguration enables
834 synthetic reductive metabolism in yeast. Nat Metab. 2022;4(11):1551-9. Epub 20221027. doi:
835 10.1038/s42255-022-00654-1. PubMed PMID: 36302903; PubMed Central PMCID:
836 PMCPMC9684072.

837 30. Rongpipi S, Ye D, Gomez ED, Gomez EW. Progress and opportunities in the
838 characterization of cellulose - an important regulator of cell wall growth and mechanics. Front
839 Plant Sci. 2018;9:1894. Epub 2019/03/19. doi: 10.3389/fpls.2018.01894. PubMed PMID:
840 30881371; PubMed Central PMCID: PMCPMC6405478.
841 31. Dinh HV, Suthers PF, Chan SHJ, Shen Y, Xiao T, Deewan A, et al. A comprehensive
842 genome-scale model for *Rhodosporidium toruloides* IFO0880 accounting for functional
843 genomics and phenotypic data. Metab Eng Commun. 2019;9:e00101. Epub 20190828. doi:
844 10.1016/j.mec.2019.e00101. PubMed PMID: 31720216; PubMed Central PMCID:
845 PMCPMC6838544.
846 32. Coradetti ST, Craig JP, Xiong Y, Shock T, Tian C, Glass NL. Conserved and essential
847 transcription factors for cellulase gene expression in ascomycete fungi. Proc Natl Acad Sci U S
848 A. 2012;109(19):7397-402.
849 33. Stricker AR, Grosstessner-Hain K, Würleitner E, Mach RL. Xyr1 (xylanase regulator 1)
850 regulates both the hydrolytic enzyme system and D-xylose metabolism in *Hypocrea jecorina*.
851 Eukaryot Cell. 2006;5(12):2128-37. Epub 2006/10/24. doi: 10.1128/ec.00211-06. PubMed
852 PMID: 17056741; PubMed Central PMCID: PMCPMC1694815.
853 34. Li Z, Yao G, Wu R, Gao L, Kan Q, Liu M, et al. Synergistic and dose-controlled
854 regulation of cellulase gene expression in *Penicillium oxalicum*. PLoS Genet.
855 2015;11(9):e1005509. Epub 2015/09/12. doi: 10.1371/journal.pgen.1005509. PubMed PMID:
856 26360497; PubMed Central PMCID: PMC4567317.
857 35. van Peij NN, Gielkens MM, de Vries RP, Visser J, de Graaff LH. The transcriptional
858 activator XlnR regulates both xylanolytic and endoglucanase gene expression in *Aspergillus*
859 *niger*. Appl Environ Microbiol. 1998;64(10):3615-9. Epub 1998/10/06. PubMed PMID: 9758775;
860 PubMed Central PMCID: PMC106473.
861 36. Price MN, Dehal PS, Arkin AP. FastTree 2--approximately maximum-likelihood trees for
862 large alignments. PLoS One. 2010;5(3):e9490. Epub 2010/03/13. doi:

863 10.1371/journal.pone.0009490. PubMed PMID: 20224823; PubMed Central PMCID:
864 PMCPMC2835736.
865 37. Samal A, Craig JP, Coradetti ST, Benz JP, Eddy JA, Price ND, et al. Network
866 reconstruction and systems analysis of plant cell wall deconstruction by *Neurospora crassa*.
867 Biotechnol Biofuels. 2017;10:225. Epub 2017/09/28. doi: 10.1186/s13068-017-0901-2. PubMed
868 PMID: 28947916; PubMed Central PMCID: PMCPMC5609067.
869 38. Bhat PJ, Murthy TV. Transcriptional control of the GAL/MEL regulon of yeast
870 *Saccharomyces cerevisiae*: mechanism of galactose-mediated signal transduction. Mol
871 Microbiol. 2001;40(5):1059-66. doi: 10.1046/j.1365-2958.2001.02421.x. PubMed PMID:
872 11401712.
873 39. Kanehisa M, Goto S. KEGG: Kyoto encyclopedia of genes and genomes. Nucleic Acids
874 Res. 2000;28(1):27-30. Epub 1999/12/11. doi: 10.1093/nar/28.1.27. PubMed PMID: 10592173;
875 PubMed Central PMCID: PMCPMC102409.
876 40. Ashburner M, Ball CA, Blake JA, Botstein D, Butler H, Cherry JM, et al. Gene ontology:
877 tool for the unification of biology. The Gene Ontology Consortium. Nat Genet. 2000;25(1):25-9.
878 doi: 10.1038/75556. PubMed PMID: 10802651; PubMed Central PMCID: PMCPMC3037419.
879 41. Gene Ontology Consortium. The Gene Ontology knowledgebase in 2026. Nucleic Acids
880 Res. 2025. Epub 20251218. doi: 10.1093/nar/gkaf1292. PubMed PMID: 41413728.
881 42. Madeira F, Madhusoodanan N, Lee J, Eusebi A, Niewielska A, Tivey ARN, et al. The
882 EMBL-EBI Job Dispatcher sequence analysis tools framework in 2024. Nucleic Acids Res.
883 2024;52(W1):W521-W5. doi: 10.1093/nar/gkae241. PubMed PMID: 38597606; PubMed Central
884 PMCID: PMCPMC11223882.
885 43. Nora LC, Wehrs M, Kim J, Cheng JF, Tarver A, Simmons BA, et al. A toolset of
886 constitutive promoters for metabolic engineering of *Rhodosporidium toruloides*. Microb Cell
887 Fact. 2019;18(1):117. Epub 2019/07/01. doi: 10.1186/s12934-019-1167-0. PubMed PMID:
888 31255171; PubMed Central PMCID: PMCPMC6599526.

889 44. Megnet R. Mutants partially deficient in alcohol dehydrogenase in *Schizosaccharomyces*
890 *pombe*. Arch Biochem Biophys. 1967;121(1):194-201. Epub 1967/07/01. doi: 10.1016/0003-
891 9861(67)90024-0. PubMed PMID: 4291962.
892 45. Marian IM, Vonk PJ, Valdes ID, Barry K, Bostock B, Carver A, et al. The transcription
893 factor Roc1 is a key regulator of cellulose degradation in the wood-decaying mushroom
894 *Schizophyllum commune*. mBio. 2022;13(3):e0062822. Epub 20220523. doi:
895 10.1128/mbio.00628-22. PubMed PMID: 35604096; PubMed Central PMCID:
896 PMCPMC9239231.
897 46. Wang Z, Li Y, Qiu H, Li Z, Ji T, Ren A, et al. GlSlt2 positively regulates GlMyb-mediated
898 cellulose utilization in *Ganoderma lucidum*. mBio. 2025;16(10):e0181225. Epub 20250908. doi:
899 10.1128/mbio.01812-25. PubMed PMID: 40919811; PubMed Central PMCID:
900 PMCPMC12506057.
901 47. Craig JP, Coradetti ST, Starr TL, Glass NL. Direct target network of the *Neurospora*
902 *crassa* plant cell wall deconstruction regulators CLR-1, CLR-2, and XLR-1. mBio.
903 2015;6(5):e01452-15. Epub 2015/10/16. doi: 10.1128/mBio.01452-15. PubMed PMID:
904 26463163; PubMed Central PMCID: PMC4620465.
905 48. Benocci T, Aguilar-Pontes MV, Kun RS, Seiboth B, de Vries RP, Daly P. ARA1 regulates
906 not only L-arabinose but also D-galactose catabolism in *Trichoderma reesei*. FEBS Lett.
907 2018;592(1):60-70. Epub 2017/12/08. doi: 10.1002/1873-3468.12932. PubMed PMID:
908 29215697.
909 49. Hynes MJ, Murray SL, Duncan A, Khew GS, Davis MA. Regulatory genes controlling
910 fatty acid catabolism and peroxisomal functions in the filamentous fungus *Aspergillus nidulans*.
911 Eukaryot Cell. 2006;5(5):794-805. Epub 2006/05/10. doi: 10.1128/ec.5.5.794-805.2006.
912 PubMed PMID: 16682457; PubMed Central PMCID: PMCPMC1459687.
913 50. Arentshorst M, Reijngoud J, Van Tol DJ, Reid ID, Arendsen Y, Pel HJ, et al. Utilization of
914 ferulic acid in *Aspergillus niger* requires the transcription factor FarA and a newly identified Far-

915 like protein (FarD) that lacks the canonical Zn (II) 2Cys6 domain. Frontiers in Fungal Biology.
916 2022;3:978845.
917 51. White AM, Mitchell AP. Control of citrate utilization by *Candida albicans* Adr1. mSphere.
918 2025;10(7):e0031125. Epub 20250611. doi: 10.1128/msphere.00311-25. PubMed PMID:
919 40497710; PubMed Central PMCID: PMCPMC12306173.
920 52. Show PL, Oladele KO, Siew QY, Aziz Zakry FA, Lan JC-W, Ling TC. Overview of citric
921 acid production from *Aspergillus niger*. Frontiers in life science. 2015;8(3):271-83.
922 53. Gallmetzer M, Meraner J, Burgstaller W. Succinate synthesis and excretion by
923 *Penicillium simplicissimum* under aerobic and anaerobic conditions. FEMS Microbiol Lett.
924 2002;210(2):221-5. doi: 10.1111/j.1574-6968.2002.tb11184.x. PubMed PMID: 12044678.
925 54. Yugueros SI, Peláez J, Stajich JE, Fuertes-Rabanal M, Sánchez-Vallet A, Largo-Gosens
926 A, et al. Study of fungal cell wall evolution through its monosaccharide composition: An insight
927 into fungal species interacting with plants. Cell Surf. 2024;11:100127. Epub 20240525. doi:
928 10.1016/j.tcsw.2024.100127. PubMed PMID: 38873189; PubMed Central PMCID:
929 PMCPMC11170279.
930 55. Beattie SR, Mark KMK, Thammahong A, Ries LNA, Dhingra S, Caffrey-Carr AK, et al.
931 Filamentous fungal carbon catabolite repression supports metabolic plasticity and stress
932 responses essential for disease progression. PLoS Pathog. 2017;13(4):e1006340. Epub
933 2017/04/20. doi: 10.1371/journal.ppat.1006340. PubMed PMID: 28423062; PubMed Central
934 PMCID: PMC5411099.
935 56. Ries LNA, Beattie S, Cramer RA, Goldman GH. Overview of carbon and nitrogen
936 catabolite metabolism in the virulence of human pathogenic fungi. Mol Microbiol.
937 2018;107(3):277-97. Epub 2017/12/03. doi: 10.1111/mmi.13887. PubMed PMID: 29197127;
938 PubMed Central PMCID: PMCPMC5777862.

939 57. Ospina-Giraldo MD, Mullins E, Kang S. Loss of function of the *Fusarium oxysporum*
940 *SNF1* gene reduces virulence on cabbage and *Arabidopsis*. Curr Genet. 2003;44(1):49-57.
941 Epub 2003/07/08. doi: 10.1007/s00294-003-0419-y. PubMed PMID: 12845476.
942 58. Zhang S, Ito M, Skerker JM, Arkin AP, Rao CV. Metabolic engineering of the oleaginous
943 yeast *Rhodosporidium toruloides* IFO0880 for lipid overproduction during high-density
944 fermentation. Appl Microbiol Biotechnol. 2016;100(21):9393-405. Epub 2016/09/30. doi:
945 10.1007/s00253-016-7815-y. PubMed PMID: 27678117.
946 59. Abbott EP, Ianiri G, Castoria R, Idnurm A. Overcoming recalcitrant transformation and
947 gene manipulation in Pucciniomycotina yeasts. Appl Microbiol Biotechnol. 2013;97(1):283-95.
948 Epub 20121114. doi: 10.1007/s00253-012-4561-7. PubMed PMID: 23149757.
949 60. Colot HV, Park G, Turner GE, Ringelberg C, Crew CM, Litvinkova L, et al. A high-
950 throughput gene knockout procedure for *Neurospora* reveals functions for multiple transcription
951 factors. Proc Natl Acad Sci U S A. 2006;103(27):10352-7. Epub 2006/06/28. doi:
952 10.1073/pnas.0601456103. PubMed PMID: 16801547; PubMed Central PMCID: PMC1482798.
953 61. McCluskey K, Wiest A, Plamann M. The Fungal Genetics Stock Center: a repository for
954 50 years of fungal genetics research. J Biosci. 2010;35(1):119-26. Epub 2010/04/24. PubMed
955 PMID: 20413916.
956 62. Vogel H. A convenient growth medium for *Neurospora* (medium N). Microbial Genetics
957 Bulletin. 1956;13(4):42-3.
958 63. Grigoriev IV, Nikitin R, Haridas S, Kuo A, Ohm R, Otillar R, et al. MycoCosm portal:
959 gearing up for 1000 fungal genomes. Nucleic Acids Res. 2014;42(Database issue):D699-704.
960 Epub 2013/12/04. doi: 10.1093/nar/gkt1183. PubMed PMID: 24297253; PubMed Central
961 PMCID: PMCPMC3965089.
962 64. Edgar RC. MUSCLE: multiple sequence alignment with high accuracy and high
963 throughput. Nucleic Acids Res. 2004;32(5):1792-7. Epub 20040319. doi: 10.1093/nar/gkh340.
964 PubMed PMID: 15034147; PubMed Central PMCID: PMCPMC390337.

965 65. Tamura K, Stecher G, Kumar S. MEGA11: Molecular Evolutionary Genetics Analysis
966 Version 11. Mol Biol Evol. 2021;38(7):3022-7. doi: 10.1093/molbev/msab120. PubMed PMID:
967 33892491; PubMed Central PMCID: PMCPMC8233496.
968 66. Patro R, Duggal G, Love MI, Irizarry RA, Kingsford C. Salmon provides fast and bias-
969 aware quantification of transcript expression. Nat Methods. 2017;14(4):417-9. Epub 2017/03/07.
970 doi: 10.1038/nmeth.4197. PubMed PMID: 28263959; PubMed Central PMCID:
971 PMCPMC5600148.
972 67. Dobin A, Davis CA, Schlesinger F, Drenkow J, Zaleski C, Jha S, et al. STAR: ultrafast
973 universal RNA-seq aligner. Bioinformatics. 2013;29(1):15-21. Epub 20121025. doi:
974 10.1093/bioinformatics/bts635. PubMed PMID: 23104886; PubMed Central PMCID:
975 PMCPMC3530905.
976 68. Putri GH, Anders S, Pyl PT, Pimanda JE, Zanini F. Analysing high-throughput
977 sequencing data in Python with HTSeq 2.0. Bioinformatics. 2022;38(10):2943-5. doi:
978 10.1093/bioinformatics/btac166. PubMed PMID: 35561197; PubMed Central PMCID:
979 PMCPMC9113351.
980 69. Love MI, Huber W, Anders S. Moderated estimation of fold change and dispersion for
981 RNA-seq data with DESeq2. Genome Biol. 2014;15(12):550. Epub 2014/12/18. doi:
982 10.1186/s13059-014-0550-8. PubMed PMID: 25516281; PubMed Central PMCID:
983 PMCPMC4302049.
984 70. Xu S, Hu E, Cai Y, Xie Z, Luo X, Zhan L, et al. Using clusterProfiler to characterize
985 multiomics data. Nat Protoc. 2024;19(11):3292-320. Epub 20240717. doi: 10.1038/s41596-024-
986 01020-z. PubMed PMID: 39019974.
987 71. Lenth RVP, J. emmeans: Estimated Marginal Means, aka Least-Squares Means. R
988 package version 2.0.1 ed2025.
989